A global–local approach to the high-fidelity impact analysis of composite structures based on node-dependent kinematics

A global-local approach to the high-fidelity impact analysis of composite structures based on node-dependent kinematics

M.H. Nagaraj[1], E. Carrera[1,2], and M. Petrolo[1]

[1]MUL[2] Lab, Department of Mechanical and Aerospace Engineering, Politecnico di Torino, Corso Duca degli Abruzzi 24, 10129 Torino, Italy
[2]Department of Mechanical Engineering, Prince Mohammad Bin Fahd University, Saudi Arabia

Submitted to Composite Structures: Revised Manuscript COMSTR-D-22-02895

Author for correspondence:
M.H. Nagaraj
e-mail: Manish_Nagaraj@uml.edu

Abstract

The objective of the present work is to investigate progressive damage in fibre-reinforced composites under varying load conditions, and in particular transverse impact loads, using a global-local approach. The numerical models are built using higher-order structural theories based on the Carrera Unified Formulation (CUF). The node-dependent kinematics (NDK) technique, an intrinsic feature of CUF models, is employed which enables the selective refinement of critical regions of interest within the structure and results in a global-local analysis. Progressive damage is governed by the CODAM2 material model, which is based on continuum damage mechanics. A series of numerical assessments are performed on composite laminates under varying load conditions, and predicted results of the global-local analysis are found to be in good agreement with experimental data, thereby validating the proposed approach. A comparison of its performance with reference high-fidelity CUF models of the full structure demonstrates the computational efficiency that can be achieved using the CUF-NDK global-local approach.

Keywords: global-local analysis, composite damage, low-velocity impact, CUF

1 Introduction

Composite materials have gained significant traction within the aerospace sector over the past few decades due to their properties such as high specific stiffness and strength. Physical testing as a design and analysis tool is often impractical due to the large design space associated with this class of materials. This issue, and the availability of high-performance computing, has led to the emergence of computational techniques as a viable alternative to physical testing.

Composites, however, feature multiple failure modes under varying load conditions and lead to a very nonlinear response at the structural scale. Sophisticated material models are therefore required within the computational analysis to simulate progressive damage and eventual failure. Such material models often require accurate stress and strain fields as inputs, and necessitate very refined 3D numerical models [1]. Due to these requirements, the progressive damage analysis of composite structures is often a computationally demanding task. This is especially true in cases such as impact analysis where the presence of multiple sources of nonlinearity results in a complex numerical problem, leading to run-times in terms of hours and days even on modern parallel computing systems [2, 3]. The issue of computational cost poses a limitation on the use of virtual testing approaches, and must be addressed in order to better utilise the potential of composite material systems in engineering applications.

Several approaches have been proposed in the literature to reduce the computational effort required for the nonlinear analysis of composite structures. In general, these approaches make use of the global-local technique where only the critical region of interest within the model is refined, while the remaining zones are modelled in low-fidelity [4]. The selective refinement strategy is achieved using various techniques, specifically when applied to complex problems involving composite damage. A popular technique is solid/shell coupling in which the critical (local) zone is modelled in 3D while the non-critical (global) region is modelled in 2D, with tie-constraints connecting the two regions, and can be solved simultaneously in a single analysis. This technique has been applied to problems such as stiffener-skin debonding [5], and the low-velocity impact analysis of composite laminates [6, 7]. Similarly, the submodeling feature available in commercial FE platforms has been applied to study buckling and damage behaviour in stiffened composite panels [8], and has been extended to the debonding and progressive failure analysis of these structures [9]. Another approach to global-local analysis relies on the Arlequin method [10]. This approach allows for the coupling of two volumes with different mechanical states, usually via the use of Lagrange multipliers, and has been successfully used to bridge low- and high-fidelity meshes within a single finite element analysis [11, 12]. More recently, neural networks have been employed to develop an FEA-based global-local technique [13].

This paper presents an investigation into the global-local progressive damage analysis of composite structures using higher-order structural based on the Carrera Unified Formulation (CUF) [14]. Within this numerical approach, the capabilities of 1D and 2D finite elements are enhanced by the use of additional expansion functions, resulting in a 3D definition of the displacement field, and consequently, strain and stress fields. This leads to

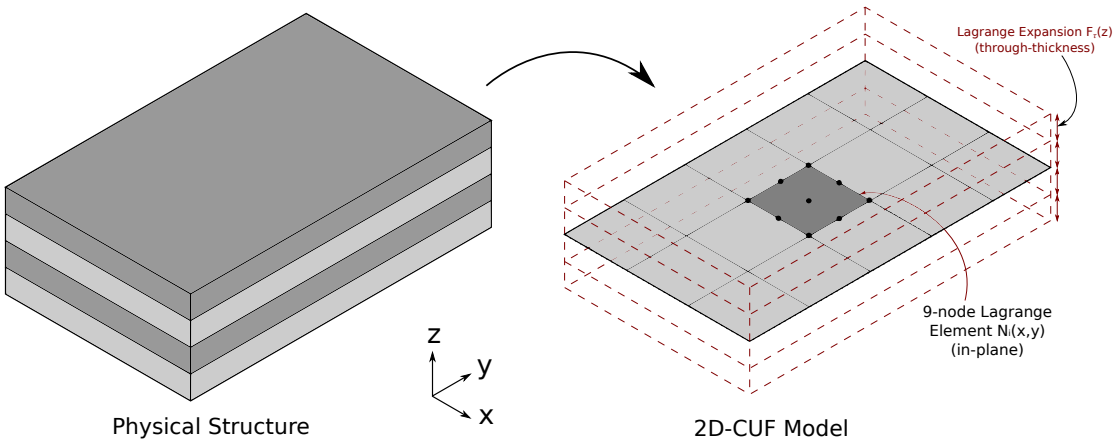

Figure 1: Layer-wise modelling of composite laminates in CUF.

a solution accuracy approaching that of 3D finite element analysis (FEA) at reduced computational effort [15]. The capabilities of CUF models have been successfully demonstrated for problems such as the geometrically nonlinear analysis of composite beams [16–18], contact modelling [19, 20], progressive damage and impact analysis [21–23], and micromechanical and multiscale analysis [24–26]. In recent years, CUF models have also been interfaced with commercial FE platforms to derive a global-local technique and has been applied to linear analysis [27], as well as nonlinear problems such as elastoplasticity and progressive damage [28, 29]. The current work investigates progressive damage analysis by utilising the node-dependent kinematics (NDK) capability of the CUF framework, wherein variable kinematic approximations can be used in different regions of the structural model. This approach allows for the development of a single numerical model with high-fidelity local zones and a low-fidelity model of the remaining global structure, leading to a global-local model which is solved in a single step.

The organisation of this paper is as follows: Section 2 provides an overview of the structural and material modelling approach. A set of numerical assessments are presented as verification and validation cases in Section 3, while the major conclusions are summarised in Section 4.

2 Numerical modelling

2.1 Structural theories and FE formulation

Considering a generalised multi-layered structure as shown in Fig. 1, the displacement field for layer-wise CUF models is defined as

$$\mathbf{u}(x,y,z) = F_\tau(z)\mathbf{u}_\tau(x,y), \tau = 1,2,\dots M \tag{1}$$

where $F_\tau(z)$ is a 1D interpolative function in the thickness direction, and is termed the expansion function. M represents the terms within $F_\tau(z)$, and $\mathbf{u}_\tau(x,y)$ is the generalized in-plane displacement. The current work

employs Lagrange polynomials as the choice of $F_\tau(z)$, and is termed Lagrange Expansion (LEp), where p denotes the polynomial order. The use of LE leads to the development of a layer-wise model which contains only displacement degrees of freedom (DOF). Further details of layer-wise modelling in CUF is found in [14]

Finite element formulation

The 3D stress and strain fields are represented in vector form as

$$\begin{aligned} \boldsymbol{\sigma} &= \{\sigma_{xx}, \sigma_{yy}, \sigma_{zz}, \sigma_{xy}, \sigma_{xz}, \sigma_{yz}\} \\ \boldsymbol{\varepsilon} &= \{\varepsilon_{xx}, \varepsilon_{yy}, \varepsilon_{zz}, \varepsilon_{xy}, \varepsilon_{xz}, \varepsilon_{yz}\} \end{aligned} \tag{2}$$

Assuming infinitesimal strains, the displacement-strain relation is

$$\boldsymbol{\varepsilon} = \mathbf{D}\mathbf{u} \tag{3}$$

where $\mathbf{u}$ is the displacement vector and $\mathbf{D}$ is the linear differential operator, defined as

$$\mathbf{D} = \begin{bmatrix} \frac{\partial}{\partial x} & 0 & 0 \\ 0 & \frac{\partial}{\partial y} & 0 \\ 0 & 0 & \frac{\partial}{\partial z} \\ \frac{\partial}{\partial y} & \frac{\partial}{\partial x} & 0 \\ \frac{\partial}{\partial z} & 0 & \frac{\partial}{\partial x} \\ 0 & \frac{\partial}{\partial z} & \frac{\partial}{\partial y} \end{bmatrix}$$

The constitutive relation, considering physical nonlinearity, t is given by

$$\boldsymbol{\sigma} = \mathbf{C}^{sec}\boldsymbol{\varepsilon} \tag{4}$$

where $\mathbf{C}^{sec}$ is the secant stiffness matrix obtained from the composite damage model used in the analysis. Quadratic 9-node 2D finite elements, termed as Q9 elements, with shape functions $N_i(x, y)$ are used to discretise the in-plane geometry, and in combination with the through-thickness expansion function $F_\tau(z)$, result in the following 3D displacement field

$$\mathbf{u}(x, y, z) = N_i(x, y)F_\tau(z)\mathbf{u}_{\tau i} \tag{5}$$

The semi-discrete balance of momentum is

$$\mathbf{M}\ddot{\mathbf{u}} = \mathbf{F}_{ext} - \mathbf{F}_{int} \tag{6}$$

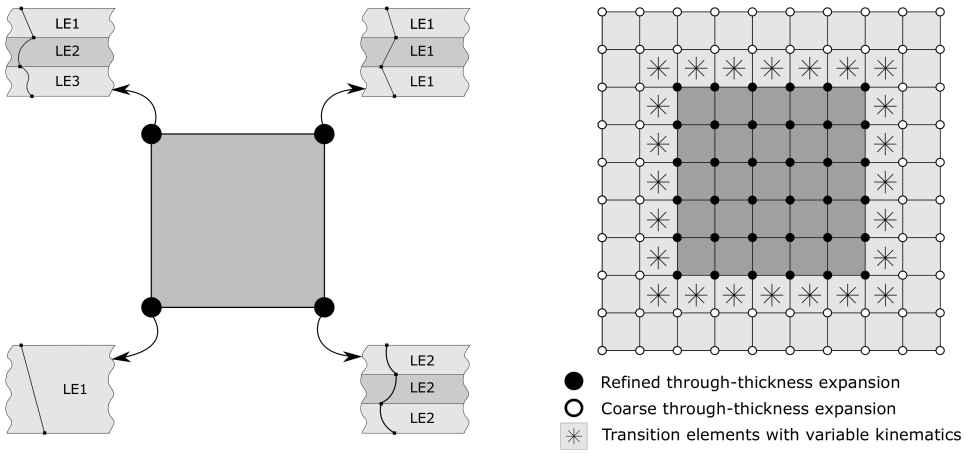

(a) Node-dependent kinematics (b) Global-local analysis using NDK

Figure 2: Node-dependent kinematic (NDK) approach in CUF and its application to global-local analysis.

where $\mathbf{M}$ and $\ddot{\mathbf{u}}$ are the mass matrix and the acceleration vector, respectively. The external force vector is denoted by $\mathbf{F}_{ext}$ and $\mathbf{F}_{int}$ is the vector of internal forces. Equation 6 is solved using explicit time integration, and a detailed overview of the development of a nonlinear explicit dynamics framework based on CUF structural theories is found in [21].

2.2 Node-dependent kinematics

The manner in which the 3D displacement field is defined within 2D-CUF (see Eq. 5), i.e. as a combination of the 2D shape functions $N_i(x, y)$ and 1D expansion functions $F_\tau(z)$, allows for the use of variable kinematics within the structural model. This is formally termed as Node-Dependent Kinematics (NDK), wherein the nodes of a finite element may be prescribed different expansion functions, as seen in Fig. 2(a). Within this approach, different 1D thickness expansion functions (F_τ) prescribed on the FE nodes can be integrated within the same 2D finite element via the nodal shape functions. A detailed description and formulation of NDK within 1D- and 2D-CUF theories is found in [30, 31]

The capability of assigning variable kinematics at the nodal level leads to a flexible structural modelling approach where different regions of the structure can be modelled with varying levels of fidelity. This can be utilised to enable global-local analysis within a single numerical model, as seen in Fig. 2(b), where the highlighted local region of interest is prescribed a refined (high-fidelity) through-thickness expansion, while the remaining global structure is modelled with a coarser (low-fidelity) expansion through its thickness. The two disparate regions are connected through a layer of node-dependent kinematic elements, each consisting of both coarse and refined thickness expansion functions at the FE nodes and serving as a transition zone between the coarse and refined meshes, as illustrated in Fig. 2(b). The kinematic description of the NDK element is independent at the nodal level and a natural kinematic variation can thereby be obtained over the element domain, resulting in a continuous displacement field [30]. This allows for an intrinsic connection between the two zones while avoiding the need for special coupling techniques such as, for instance, the Arlequin method

applied to global-local analysis [10].

The CUF-NDK global-local approach results in an accurate evaluation of the selected zones of interest, such as critical regions in the vicinity of stress concentrators, while reducing the computational effort required in analysing the non-critical regions of the structure. Furthermore, the analysis is performed in a single step, which is in contrast to conventional global-local approaches where the low-fidelity global and high-fidelity local analyses are performed sequentially [27, 29]. In the present work, the critical (local) regions are modelled using a layer-wise approach, where each ply is represented by a Lagrange polynomial of an appropriate order, while the remaining (global) structure are modelled using an equivalent single-layer approach using a single expansion function to define the entire laminate thickness.

2.3 CODAM2 intralaminar damage model

Progressive damage within the composite laminate is governed by the continuum damage mechanics-based CODAM2 material model [32, 33]. This model has been previously combined with layer-wise 2D-CUF models to investigate tensile and progressive damage [21, 22]. A brief overview of the formulation is presented in this section. The subscripts 'T' and 'C' refer to tensile and compressive modes, respectively. Fibre damage initiation is evaluated using the maximum stress criterion as follows

$$F_1 = \frac{\sigma_{11}}{X_{T/C}} \tag{7}$$

where $X_{T/C}$ denotes the fibre (tensile/compressive) strength, and σ_{11} is the stress in the fibre direction. The indices $11, 22, 12$ indicate fields in the material reference system. Damage initiation transverse to the fibre, i.e. matrix damage initiation, is evaluated using Hashin's quadratic failure criterion [34]

$$F_2 = \left(\frac{\sigma_{22}}{Y_{T/C}}\right)^2 + \left(\frac{\tau_{12}}{S_L}\right)^2 \tag{8}$$

where $Y_{T/C}$ is the transverse strength and S_L is the in-plane shear strength. Equivalent strains can be defined in the longitudinal and transverse directions as

$$\varepsilon_1^{eq} = |\varepsilon_{11}| \tag{9}$$

$$\varepsilon_2^{eq} = \sqrt{(\gamma_{12})^2 + (\varepsilon_{22})^2} \tag{10}$$

where subscripts 1 and 2 respectively indicate the longitudinal (fibre) and transverse (matrix) directions. The corresponding equivalent stress measures are given by

$$\sigma_1^{eq} = \sigma_{11} \tag{11}$$

$$\sigma_2^{eq} = \frac{\tau_{12}\gamma_{12} + \sigma_{22}\varepsilon_{22}}{\sqrt{(\gamma_{12})^2 + (\varepsilon_{22})^2}} \tag{12}$$

The equivalent strain measures at damage initiation are

$$\varepsilon_\alpha^i = \varepsilon_\alpha^{eq}|_{F_\alpha=1}, \quad \alpha = 1, 2 \tag{13}$$

The strains at damage saturation are quantified as

$$\varepsilon_1^s = \frac{2g_1^f}{X_{T/C}} \quad and \quad \varepsilon_2^s = \frac{2g_2^f}{T} \tag{14}$$

where $T = \sigma_2^{eq}|_{F_2=1}$ is the value of σ_2^{eq} at matrix damage initiation. Mesh dependency is addressed by applying the crack-band theory [35], where the experimentally-obtained fracture energy G_α^f is scaled using a characteristic length parameter l^* to obtain the fracture energy density g_α^f as follows

$$g_\alpha^f = \frac{G_\alpha^f}{l^*}, \quad \alpha = 1, 2 \tag{15}$$

The present work uses a characteristic length $l^* = (V_{GP})^{\frac{1}{3}}$, where V_{GP} is the volume associated with the Gauss point of the element. The damage parameters ω_1 and ω_2 are then computed as

$$\omega_\alpha = \left(\frac{\langle \varepsilon_\alpha^{eq} - \varepsilon_\alpha^i \rangle}{\varepsilon_\alpha^s - \varepsilon_\alpha^i}\right)\left(\frac{\varepsilon_\alpha^s}{\varepsilon_\alpha^{eq}}\right), \quad \alpha = 1, 2 \tag{16}$$

where $\langle\cdot\rangle$ denotes the Macauley bracket. The stiffness reduction factors, R_α, are computed as

$$R_\alpha = (1 - \omega_\alpha), \quad \alpha = 1, 2 \tag{17}$$

The secant material stiffness matrix can then be evaluated as

$$\mathbf{C}^{dam} = \frac{1}{\Delta}\begin{bmatrix} (1 - R_2\nu_{23}\nu_{32})R_1E_1 & (\nu_{21} + \nu_{23}\nu_{31})R_1R_2E_1 & (\nu_{31} + R_2\nu_{21}\nu_{32})R_1E_1 & 0 & 0 & 0 \\ & (1 - R_1\nu_{31}\nu_{13})R_2E_2 & (\nu_{32} + R_1\nu_{31}\nu_{12})R_2E_2 & 0 & 0 & 0 \\ & & (1 - R_1R_2\nu_{21}\nu_{12})E_3 & 0 & 0 & 0 \\ & & & \Delta R_1R_2G_{12} & 0 & 0 \\ & sym. & & & \Delta G_{23} & 0 \\ & & & & & \Delta G_{13} \end{bmatrix} \tag{18}$$

where $\Delta = 1 - R_2\nu_{23}\nu_{32} - R_1R_2\nu_{12}\nu_{21} - 2R_1R_2\nu_{31}\nu_{12}\nu_{23} - R_1\nu_{31}\nu_{13}$. The 3D stress state is then computed as follows

$$\boldsymbol{\sigma} = \mathbf{C}^{dam}\boldsymbol{\varepsilon} \tag{19}$$

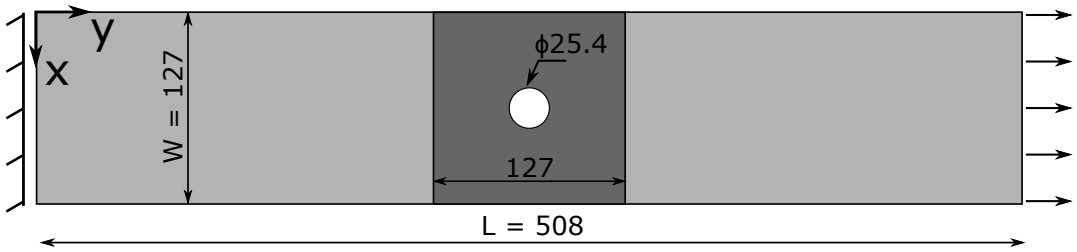

Figure 3: Schematic representation of the $[45/90/-45/0]_{8s}$ open-hole tension specimen with the critical region highlighted (dimensions in mm).

Table 1: Material properties of IM7/8552 [37].

$E_1^{(T)}$ [GPa]	$E_1^{(C)}$ [GPa]	$E_{2,3}^{(T)}$ [GPa]	$E_{2,3}^{(C)}$ [GPa]	G_{12} [GPa]	G_{13} [GPa]	G_{23} [GPa]	ν_{12}	ν_{13}	ν_{23}
165.0	150.0	9.0	11.0	5.8	5.8	2.9	0.34	0.34	0.48
X_T [MPa]	X_C [MPa]	Y_T [MPa]	Y_C [MPa]	S_{12} [MPa]	G_1^T $[kJ/m^2]$	G_2^T $[kJ/m^2]$	G_1^C $[kJ/m^2]$	G_2^C $[kJ/m^2]$	
2560.0	1690.0	73.0	250.0	90.0	120.0	2.6	80.0	4.2	

3 Numerical Assessments

3.1 Tensile strength prediction of open-hole specimen

The aim of the present assessment is the strength prediction of an open-hole tensile (OHT) specimen, and is a verification of the proposed global-local technique applied to tensile damage analysis. The assessment is based on the works of Green et al. [36], which provides experimental strength measurements. The structure was previously investigated using CUF-based models and is reported in [29]. The specimen is composed of IM7/8552 carbon fibre-reinforced polymer (CFRP) with a nominal ply thickness of 0.125 mm. The elastic and strength properties of this material system are presented in Table 1. The stacking sequence is $[45/90/-45/0]_{8s}$, leading to a laminate thickness of 8 mm. The OHT specimen, with the critical region highlighted, is schematically shown in Fig. 3.

The OHT specimen is analysed using the CUF-NDK global-local approach, where each ply within the critical region (highlighted in Fig. 3) is explicitly modelled using a first-order Lagrange polynomial expansion (LE1), while the remaining global region is modelled with a single LE1 representing the laminate thickness. Three CUF models, with a progressive refinement of the in-plane discretisation using quadratic 9-node 2D finite

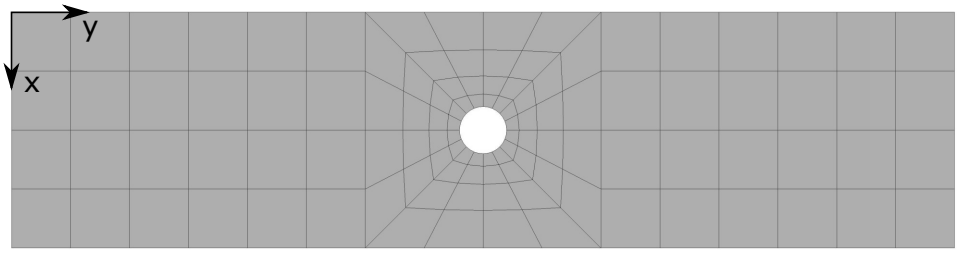

Figure 4: Schematic representation of the CUF model with 112 Q9 (quadratic, 9-node) elements for the case of the OHT specimen.

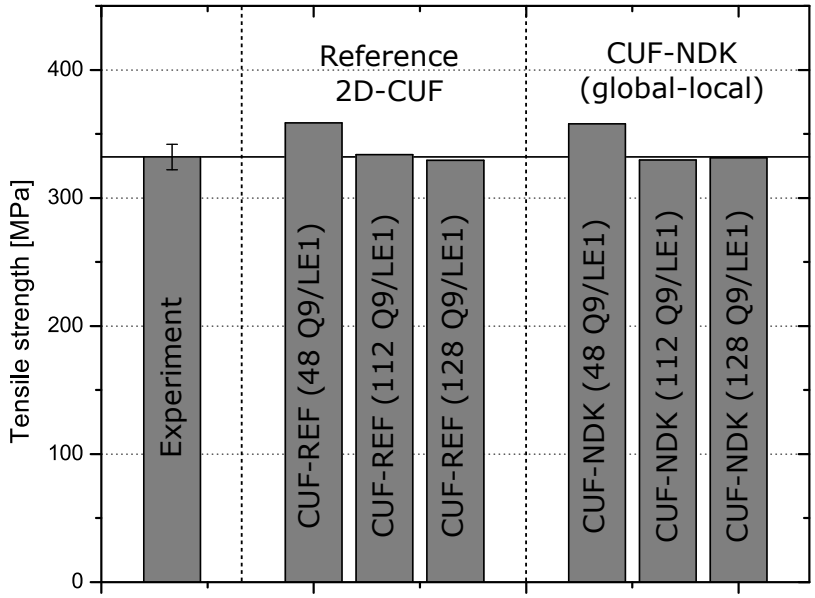

Figure 5: Tensile strength of OHT specimen predicted by the CUF-NDK global-local approach. Reference experimental results obtained from [36].

Table 2: Model information for the tensile strength prediction of $[45/90/-45/0]_{8s}$ quasi-isotropic OHT specimen.

Model	Discretisation of the open-hole specimen	DOF	Time* [hh:mm:ss]
	Reference 2D-CUF		
CUF-REF – 48Q9	48 Q9 elements in-plane (1 LE1/ply)	45,240	1:44:35
CUF-REF – 112Q9	112 Q9 elements in-plane (1 LE1/ply)	98,280	4:14:28
CUF-REF – 128Q9	128 Q9 elements in-plane (1 LE1/ply)	110,760	4:55:36
	CUF-NDK (global-local analysis)		
CUF-NDK – 48Q9	48 Q9 elements in-plane (local: 1 LE1/ply, global: 1 LE1/laminate)	22,560	0:47:56
CUF-NDK – 112Q9	112 Q9 elements in-plane (local: 1 LE1/ply, global: 1 LE1/laminate)	57,456	2:19:30
CUF-NDK – 128Q9	128 Q9 elements in-plane (local: 1 LE1/ply, global: 1 LE1/laminate)	69,936	3:04:34

* The reported run-times are based on analyses performed on a laptop using 4 cores.

elements (Q9), have been considered for the analysis. As an example, the CUF model with 112 Q9 elements is schematically shown in Fig. 4. The tensile strengths predicted by the CUF models are plotted in Fig. 5. The experimentally obtained strength [36], and the reference numerical predictions using layer-wise CUF models of the entire structure [29], are also shown for comparison. Details of the numerical models are listed in Table 2. The following observations are made:

1. Numerical models based on the CUF-NDK global-local approach successfully predict the tensile strength of the OHT specimen, as seen in Fig. 5. In particular, the predictions of the NDK models are in very good agreement with those of the reference high-fidelity CUF models.

2. Selective through-thickness refinement of the critical regions leads to a reduction in the DOF of the system and a proportional reduction in the required analysis time, as seen in Table 2.

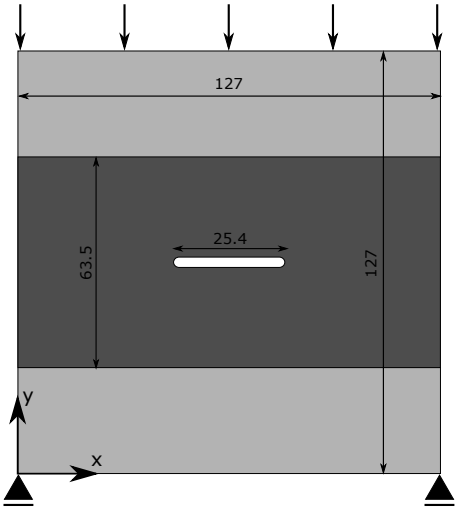

Figure 6: Schematic representation of the $[45/90/-45/0]_{4s}$ centre-notched compressive specimen with the local region highlighted (dimensions in mm).

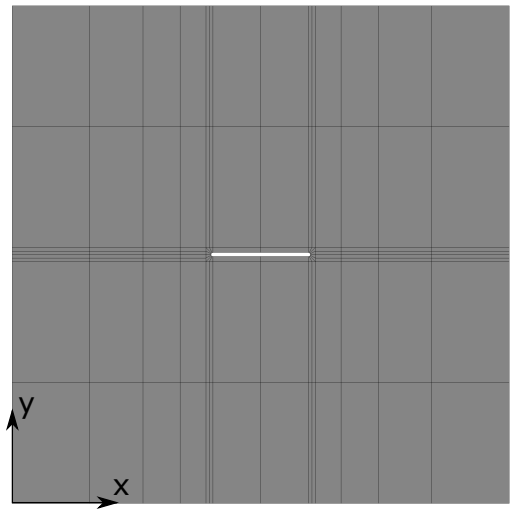

Figure 7: Schematic representation of the CUF model with 108 Q9 (quadratic, 9-node) elements for the case of the CNC specimen.

3. Comparing the coarsest CUF models which predict the tensile strength with the required accuracy, i.e. the CUF-REF and CUF-NDK models with 112 Q9 in-plane discretisation (error $< 1\%$), it is seen from Table 2 that the proposed global-local approach provides an $1.8x$ speed-up in the analysis time.

3.2 Compressive strength of centre-notched laminate

This assessment is concerned with the compressive strength prediction of a 4 mm thick quasi-isotropic $[45/90/-45/0]_{4s}$ laminate with a central notch, shown schematically in Fig. 6. The material system is IM7/8552 CFRP, whose properties are listed in Table 1. The analysis is based on the works of Xu et al. [38], which provides experimental data. The centre-notched compressive (CNC) specimen was previously analysed using layer-wise CUF models [22]. The current work applies the NDK-based global-local approach, with a selective refinement of the critical regions (highlighted in Fig. 6), to the compressive strength prediction of notched laminates.

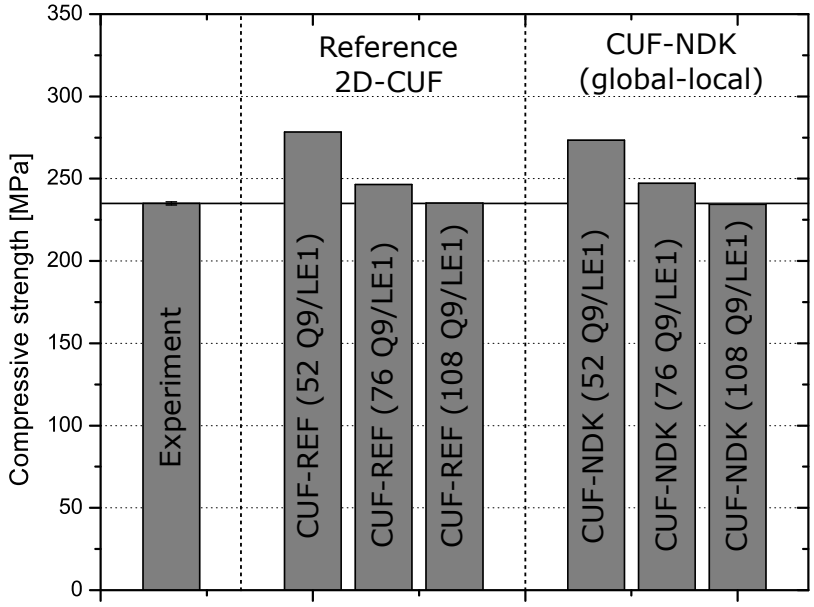

Figure 8: Compressive strength of the CNC specimen predicted by the CUF-NDK global-local approach. Reference experimental results obtained from [36].

Table 3: Model information for the compressive strength prediction of the $[45/90/-45/0]_{4s}$ quasi-isotropic CNC specimen.

Model	Discretisation of the centre-notched specimen	DOF	Time* [hh:mm:ss]
	Reference 2D-CUF		
CUF-REF – 52Q9	52 Q9 elements in-plane (1 LE1/ply)	24,552	0:43:53
CUF-REF – 76Q9	76 Q9 elements in-plane (1 LE1/ply)	34,848	1:17:22
CUF-REF – 108Q9	108 Q9 elements in-plane (1 LE1/ply)	49,104	2:58:18
	CUF-NDK (global-local analysis)		
CUF-NDK – 52Q9	52 Q9 elements in-plane (local: 1 LE1/ply, global: 1 LE1/laminate)	18,228	0:29:35
CUF-NDK – 76Q9	76 Q9 elements in-plane (local: 1 LE1/ply, global: 1 LE1/laminate)	26,106	0:43:57
CUF-NDK – 108Q9	108 Q9 elements in-plane (local: 1 LE1/ply, global: 1 LE1/laminate)	38,316	2:02:52

* The reported run-times are based on analyses performed on a laptop using 4 cores.

The CUF models are developed with a progressive refinement of the in-plane discretisation. The most refined CUF model, containing 108 Q9 (quadratic, 9-node) elements, is schematically shown in Fig. 7. As in the previous analysis, the critical region in the vicinity of the notch is modelled using a layer-wise approach, whereas the remaining global laminate thickness is represented by a single expansion. The compressive strengths predicted by the CUF-NDK models are plotted in Fig. 8, along with reference layer-wise CUF model predictions and experimental measurements for comparison. A summary of the numerical models is presented in Table 3. The following observations are made:

1. It is seen from Fig. 8 that the CUF-NDK models are capable of accurately predicting the compressive strength of the CNC specimen, thus verifying the proposed global-local approach for compressive damage analysis.

2. The reference and NDK-based CUF models with an 108 Q9 in-plane discretisation predict strengths which are in very good agreement with experimental observations (error $\sim 0.2\%$). The application of the NDK global-local technique leads to an approximately $1.5x$ improvement in the analysis time when compared to the reference CUF model.

3.3 Progressive damage analysis of a circular plate

This analysis investigates progressive damage in a circular composite laminate subjected to transverse low-velocity impact, as shown in Fig. 9. The analysis is based on the works of Shi et al. [39], which provides reference numerical and experimental data. The material system used in the analysis is HTS40/9772 CFRP, with a nominal ply thickness of 0.25 mm, and whose material properties are listed in Table 4. The laminate is composed of a $[0/90]_{2s}$ layup leading to a laminate thickness of 2.0 mm. The analysis was previously performed using layer-wise CUF models of the full structure [23], which provides a detailed description of the analysis setup.

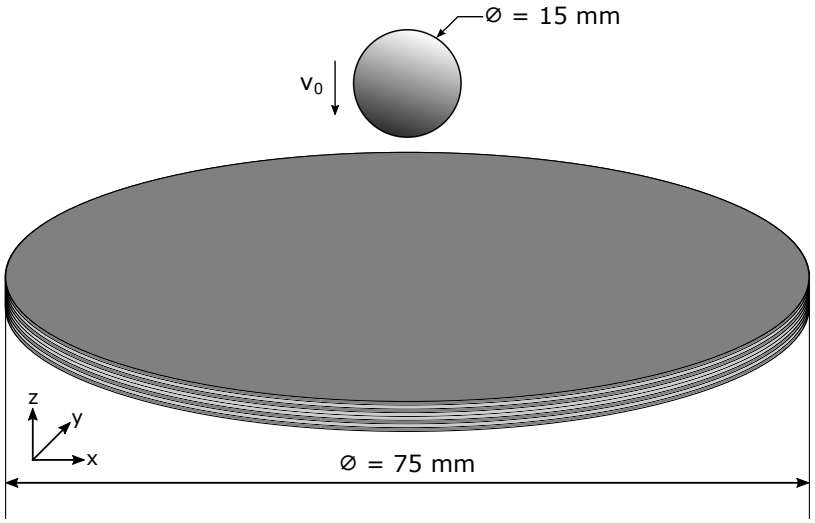

Figure 9: Schematic representation of the $[0/90]_{2s}$ composite plate under transverse low-velocity impact by a spherical indenter with a kinetic energy of 7.35 J

Table 4: Properties of the HTS40/9772 CFRP material system [39]

E_1 [GPa]	E_2 [GPa]	E_3 [GPa]	G_{12} [GPa]	G_{13} [GPa]	G_{23} [GPa]	ν_{12}	ν_{13}	ν_{23}	Density $[kg/m^3]$
153.0	10.3	10.3	6.0	6.0	3.7	0.3	0.3	0.4	1600.0
X_T [MPa]	X_C [MPa]	Y_T [MPa]	Y_C [MPa]	S_{12} [MPa]	S_{23} [MPa]	G_1^T $[kJ/m^2]$	G_2^T $[kJ/m^2]$	G_1^C $[kJ/m^2]$	G_2^C $[kJ/m^2]$
2537.0	1580.0	82.0	236.0	90.0	40.0	91.6	0.22	79.9	1.1

The impact analysis is performed using the CUF-NDK approach, where the central region under impact is modelled in a layer-wise manner with a second-order Lagrange polynomial (LE2) representing individual ply thickness. In contrast, the regions further away from the impact zone are modelled with a single expansion through the laminate thickness. The in-plane geometry is discretised using 192 quadratic finite elements (Q9),

Table 5: Properties of the cohesive layer [39]

Property	Mode I	Mode II	Mode III
Elastic modulus [GPa/mm]	1373.3	493.3	493.3
Interlaminar strength [MPa]	62.3	92.3	92.3
Interlaminar fracture toughness $[kJ/m^2]$	0.28	0.79	0.79

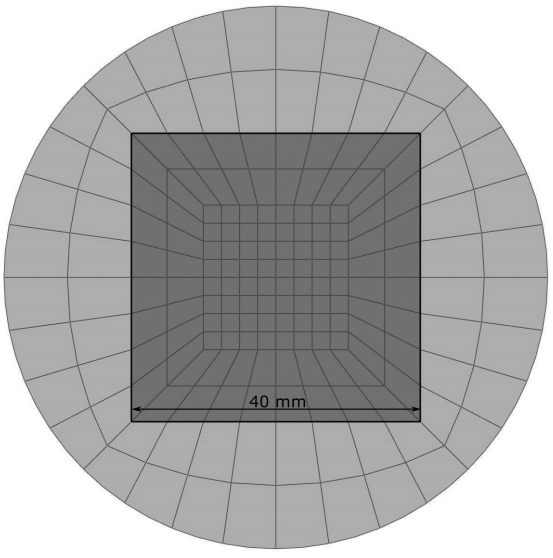

Figure 10: In-plane discretisation of the composite plate subjected to low-velocity impact, with the central region for high-fidelity analysis highlighted.

Table 6: Model information for the low-velocity impact analysis of the circular composite laminate.

Model	Discretisation of the laminate	DOF	Time* [hh:mm:ss]
	Reference 2D-CUF		
CUF-REF – 192Q9/LE1	192 Q9 elements in-plane (1 LE1/ply)	38,448	09:16:04
CUF-REF – 192Q9/LE2	192 Q9 elements in-plane (1 LE2/ply)	57,672	13:31:45
	CUF-NDK (global-local analysis)		
CUF-NDK – 192Q9	192 Q9 elements in-plane (local: 1 LE2/ply, global: 1 LE1/laminate)	40,776	08:30:09

* The reported run-times are based on analyses performed on a laptop using 4 cores.

and is determined on the basis of a mesh convergence study [23]. A schematic view of the in-plane discretisation, with the highlighted high-fidelity local region, is shown in Fig. 10. Delamination is modelled within the local high-fidelity region by inserting cohesive layers between successive CFRP plies. The cohesive properties used in the numerical models are listed in Table 5. The impact force-time response predicted by the global-local approach, with reference data based on 3D-FEA and experiments overlaid, is plotted in Fig. 11. The results obtained by reference layer-wise CUF models of the full composite plate, using LE1 and LE2 ply-thickness expansions (see Ref. [23]), are also included for comparison. A summary of all the CUF models is provided in Table 6. The following observations are made:

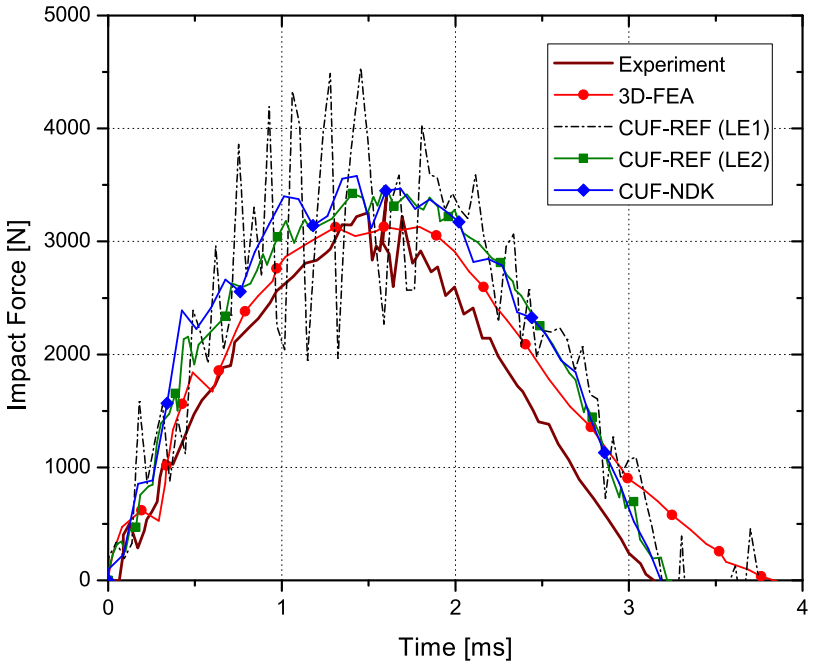

Figure 11: Impact force-time response predicted by the CUF models. Reference experimental and 3D-FEA results obtained from [39].

1. It is seen from Fig. 11 that the impact force-time curve predicted by the global-local analysis is in very good agreement with the reference CUF models, and is in good general agreement with the experimental results. This validates the proposed global-local technique for progressive damage analysis under impact loads.

2. The use of LE1 to model individual ply thickness leads to significantly oscillatory results, as seen in Fig. 11. However, applying a high-fidelity layer-wise model (using LE2) in the central impact zone, and representing the remaining regions of the laminate with a single LE1, results in a smooth response in-line with the reference data curves.

3. Comparing the computational costs between the CUF-REF (LE2) and CUF-NDK models in Table 6, it is seen that an approximately $1.6x$ speed-up in the analysis time can be achieved.

4 Conclusion

This work presents the global-local progressive damage analysis of fibre-reinforced composite structures under varying load conditions. The Carrera Unified Formulation is used to develop the numerical models, and its node-dependent kinematic feature allows for the selective through-thickness refinement of specific regions of interest within the model. The resulting numerical model consists of a high-fidelity layer-wise local region within a low-fidelity global structural model, and is solved within a single analysis. Numerical assessments are performed to predict the tensile and compressive strength of notched laminates, and the good agreement between numerical predictions and experimental observations provide an initial validation of the proposed global-local technique. The final assessment is the progressive damage analysis of a composite laminate subjected to transverse low-velocity impact. It is shown that the use of refined layer-wise kinematics in the impact zone in combination with a coarse global model leads to accurate results comparable to reference layer-wise CUF models. It is seen that an approximately $1.5x - 1.8x$ speed-up in the analysis time can be achieved, demonstrating the computational efficiency of the CUF-NDK global-local approach. This efficiency is in addition to the multi-fold improvement in analysis costs of layer-wise CUF models when compared to 3D-FEA, and is an indication of the potential of the CUF framework as a numerical tool for the design and analysis of composite structures.

Acknowledgements

This research work has been carried out within the project ICONIC (Improving the Crashworthiness of Composite Transportation Structures), funded by the European Union Horizon 2020 Research and Innovation program under the Marie Skłodowska-Curie Grant agreement No. 721256.

References

[1] YS Reddy and JN Reddy. Three-dimensional finite element progressive failure analysis of composite laminates under axial extension. *Journal of Composites, Technology and Research*, 15(2):73–87, 1993.

[2] EV González, P Maimí, PP Camanho, A Turon, and JA Mayugo. Simulation of drop-weight impact and compression after impact tests on composite laminates. *Composite Structures*, 94(11):3364–3378, 2012.

[3] G Perillo, NP Vedivik, and AT Echtermeyer. Damage development in stitch bonded gfrp composite plates under low velocity impact: Experimental and numerical results. *Journal of Composite Materials*, 49(5):601–615, 2015.

[4] AK Noor. Global-local methodologies and their application to nonlinear analysis. *Finite Elements in Analysis and Design*, 2(4):333–346, 1986.

[5] R Krueger and PJ Minguet. Analysis of composite skin–stiffener debond specimens using a shell/3d modeling technique. *Composite Structures*, 81(1):41–59, 2007.

[6] XC Sun and SR Hallett. Barely visible impact damage in scaled composite laminates: Experiments and numerical simulations. *International Journal of Impact Engineering*, 109:178–195, 2017.

[7] F Caputo, A De Luca, G Lamanna, V Lopresto, and A Riccio. Numerical investigation of onset and evolution of lvi damages in carbon–epoxy plates. *Composites Part B: Engineering*, 68:385–391, 2015.

[8] S Hühne, J Reinoso, E Jansen, and R Rolfes. A two-way loose coupling procedure for investigating the buckling and damage behaviour of stiffened composite panels. *Composite Structures*, 136:513–525, 2016.

[9] M Akterskaia, E Jansen, SR Hallett, PM Weaver, and R Rolfes. Progressive failure analysis using global-local coupling including intralaminar failure and debonding. *AIAA Journal*, pages 3078–3089, 2019.

[10] HB Dhia. Global-local approaches: the arlequin framework. *European Journal of Computational Mechanics/Revue Européenne de Mécanique Numérique*, 15(1-3):67–80, 2006.

[11] QZ He, H Hu, S Belouettar, G Guinta, K Yu, Y Liu, F Biscani, E Carrera, and M Potier-Ferry. Multi-scale modelling of sandwich structures using hierarchical kinematics. *Composite structures*, 93(9):2375–2383, 2011.

[12] Q Huang, Z Kuang, H Hu, and M Potier-Ferry. Multiscale analysis of membrane instability by using the arlequin method. *International Journal of Solids and Structures*, 162:60–75, 2019.

[13] T Yamaguchi and H Okuda. Zooming method for fea using a neural network. *Computers & Structures*, 247:106480, 2021.

[14] E Carrera, M Cinefra, M Petrolo, and E Zappino. *Finite element analysis of structures through unified formulation*. John Wiley & Sons, 2014.

[15] AG de Miguel, I Kaleel, MH Nagaraj, A Pagani, M Petrolo, and E Carrera. Accurate evaluation of failure indices of composite layered structures via various fe models. *Composites Science and Technology*, 167:174–189, 2018.

[16] A Pagani and E Carrera. Unified formulation of geometrically nonlinear refined beam theories. *Mechanics of Advanced Materials and Structures*, 25(1):15–31, 2018.

[17] Y Hui, G Giunta, G De Pietro, S Belouettar, E Carrera, Q Huang, X Liu, and H Hu. A geometrically nonlinear analysis through hierarchical one-dimensional modelling of sandwich beam structures. *Acta Mechanica*, pages 1–17, 2022.

[18] Y Hui, Q Huang, G De Pietro, G Giunta, H Hu, S Belouettar, and E Carrera. Hierarchical beam finite elements for geometrically nonlinear analysis coupled with asymptotic numerical method. *Mechanics of Advanced Materials and Structures*, 28(24):2487–2500, 2021.

[19] MH Nagaraj, I Kaleel, E Carrera, and M Petrolo. Contact analysis of laminated structures including transverse shear and stretching. *European Journal of Mechanics-A/Solids*, 80:103899, 2020.

[20] MH Nagaraj, I Kaleel, E Carrera, and M Petrolo. Nonlinear analysis of compact and thin-walled metallic structures including localized plasticity under contact conditions. *Engineering Structures*, 203:109819, 2020.

[21] MH Nagaraj, J Reiner, R Vaziri, E Carrera, and M Petrolo. Progressive damage analysis of composite structures using higher-order layer-wise elements. *Composites Part B: Engineering*, page 107921, 2020.

[22] MH Nagaraj, Johannes Reiner, R Vaziri, E Carrera, and M Petrolo. Compressive damage modeling of fiber-reinforced composite laminates using 2d higher-order layer-wise models. *Composites Part B: Engineering*, 215:108753, 2021.

[23] MH Nagaraj, E Carrera, and M Petrolo. Progressive damage analysis of composite laminates subjected to low-velocity impact using 2d layer-wise structural models. *International Journal of Non-Linear Mechanics*, 127:103591, 2020.

[24] I Kaleel, M Petrolo, AM Waas, and E Carrera. Micromechanical progressive failure analysis of fiber-reinforced composite using refined beam models. *Journal of Applied Mechanics*, 85(2), 2018.

[25] I Kaleel, M Petrolo, E Carrera, and AM Waas. Computationally efficient concurrent multiscale framework for the nonlinear analysis of composite structures. *AIAA Journal*, 57(9):4029–4041, 2019.

[26] Y Hui, R Xu, G Giunta, G De Pietro, H Hu, S Belouettar, and E Carrera. Multiscale cuf-fe2 nonlinear analysis of composite beam structures. *Computers & Structures*, 221:28–43, 2019.

[27] E Carrera, AG de Miguel, M Filippi, I Kaleel, A Pagani, M Petrolo, and Eo Zappino. Global-local plug-in for high-fidelity composite stress analysis in femap/nx nastran. *Mechanics of Advanced Materials and Structures*, pages 1–7, 2019.

[28] M Petrolo, MH Nagaraj, I Kaleel, and E Carrera. A global-local approach for the elastoplastic analysis of compact and thin-walled structures via refined models. *Computers & Structures*, 206:54–65, 2018.

[29] MH Nagaraj, M Petrolo, and E Carrera. A global–local approach for progressive damage analysis of fiber-reinforced composite laminates. *Thin-Walled Structures*, 169:108343, 2021.

[30] E Carrera, E Zappino, and G Li. Finite element models with node-dependent kinematics for the analysis of composite beam structures. *Composites Part B: Engineering*, 132:35–48, 2018.

[31] G Li, E Carrera, M Cinefra, AG De Miguel, A Pagani, and E Zappino. An adaptable refinement approach for shell finite element models based on node-dependent kinematics. *Composite structures*, 210:1–19, 2019.

[32] A Forghani, N Zobeiry, A Poursartip, and R Vaziri. A structural modelling framework for prediction of damage development and failure of composite laminates. *Journal of Composite Materials*, 47(20-21):2553–2573, 2013.

[33] J Reiner, T Feser, D Schueler, M Waimer, and R Vaziri. Comparison of two progressive damage models for studying the notched behavior of composite laminates under tension. *Composite Structures*, 207:385–396, 2019.

[34] Z Hashin. Failure criteria for unidirectional fiber composites. *Journal of applied mechanics*, 47(2):329–334, 1980.

[35] ZP Bažant and BH Oh. Crack band theory for fracture of concrete. *Matériaux et construction*, 16(3):155–177, 1983.

[36] BG Green, MR Wisnom, and SR Hallett. An experimental investigation into the tensile strength scaling of notched composites. *Composites Part A: Applied Science and Manufacturing*, 38(3):867–878, 2007.

[37] AS Kaddour, MJ Hinton, PA Smith, and S Li. Mechanical properties and details of composite laminates for the test cases used in the third world-wide failure exercise. *Journal of Composite Materials*, 47(20-21):2427–2442, 2013.

[38] X Xu, A Paul, X Sun, and MR Wisnom. An experimental study of scaling effects in notched quasi-isotropic carbon/epoxy laminates under compressive loads. *Composites Part A: Applied Science and Manufacturing*, 137:106029, 2020.

[39] Y Shi, T Swait, and C Soutis. Modelling damage evolution in composite laminates subjected to low velocity impact. *Composite Structures*, 94(9):2902–2913, 2012.